small NANO MICRO

Sensors

# Reversible Size-Tuning of Self-Assembled Silver Nanoparticles in Phospholipid Membranes via Humidity Control

*Nuri Oh, Jung Hoon Kim, Sungho Jin, and Chong Seung Yoon**

***A** monolayer of 5-nm-sized Ag nanoparticles embedded in a liquid-crystalline lipid membrane undergoes a reversible morphological change during hydration and dehydration of the lipid membrane. High mobility of the encapsulating lipid molecules, chemically bound to the Ag atoms, induces redistribution of metal particles to produce significant and optically detectable changes in nanoparticle morphology. The morphological change occurs on a time scale that enables the Ag-nanoparticle-embedded membrane to be used as a convenient visual sensor for moisture and other organic solvents, as well as for biosensing by virtue of the biocompatibility of the lipid molecules. The mechanism demonstrated here can also be extended to construct guided nanostructures based on self-assembled nanoparticles.*

**Keywords:**
- membranes
- nanoparticles
- phospholipids
- silver
- size-tuning

## 1. Introduction

In recent years, there has been rising interest in utilizing natural biomolecules such as crystalline S-layer proteins and ferritin protein cages as templates to scaffold inorganic nanostructures[1] because nature often provides striking examples of highly ordered microscopic structures formed by simple and efficient methods. Phospholipids, being amphiphilic due to the presence of both a polar head and an aliphatic tail, are capable of spontaneously arranging themselves along a phase boundary or external surface.[2] Such characteristics allow the construction of a multitude of micro- and nanostructures ranging from micelles, vesicles, and bilayers to microtubules and nanotubes. The amphilicity also renders the phospholipid able to facilitate the self-assembly of metal nanoparticles.[3] Lipid nanotubes and a solid-supported lipid multilayer were utilized to induce self-assembly of the metal particles.[4–6] In our previous work, a solid-supported lipid membrane was used as a template to synthesize nanosized Ag particles, which forced encapsulation of the resulting nanoparticles with lipid molecules.[7]

In this paper, we propose a method of tuning the morphology of the synthesized Ag nanoparticles at will by utilizing the structural change in the lipid multilayer triggered by hydration. Because the flexible lipid membrane exhibits the typical properties of a lyotropic liquid-crystalline state, the lipid structure undergoes a phase transition with increasing level of hydration.[8,9] Therefore, such a hydration-induced phase transition of the lipid membrane could force morphological changes of the embedded metal nanoparticles. We demonstrate that lipid molecules in a liquid-crystalline state can induce reversible changes in both shape and size distribution of the embedded Ag nanoparticles. The essence of our discovery is that the high mobility of encapsulating lipid molecules chemically linked to the Ag atoms enables a rapid redistribution of metal nanoparticles to produce reversible and cyclic changes in nanoparticle morphology.

## 2. Results and Discussion

Solid-supported 1,2-dioleoyl-sn-glycero-3-phosphatidylcholine (DOPC) membrane was prepared by spin-coating the lipid solution onto a Si (or fused silica) substrate following

[*] Prof. C. S. Yoon, N. Oh, J. H. Kim
Division of Materials Science Engineering, Hanyang University
17 Haengdang-dong, Seongdong-ku, Seoul (Korea)
E-mail: csyoon@hanyang.ac.kr
Prof. S. Jin
UCSD Materials Science & Engineering Program
Department of Mechanical & Aerospace Engineering
University of California at San Diego
La Jolla, California 92093 (USA)

Supporting Information is available on the WWW under http://www.small-journal.com or from the author.

DOI: 10.1002/smll.200801536

the method devised by Mennicke and Salditt.[10] A 3-nm-thick Ag layer was deposited onto the lipid multilayer using a thermal evaporator. Figure 1 shows a transmission electron microscopy (TEM) plan-view image of Ag nanoparticles produced by depositing the Ag layer directly onto the DOPC membrane. Discrete Ag nanoparticles formed a monolayer embedded within the DOPC membrane. As can be seen from the TEM image, nanoparticles with nearly spherical shapes are uniformly dispersed although some of the particles appear elongated as a result of some localized agglomeration. The electron diffraction pattern in the inset of Figure 1a was indexed to a face-centered cubic (fcc) structure with a lattice parameter of 4.1 nm, verifying that the particles are composed of metallic Ag. A cross-sectional TEM image in Figure 1b of the DOPC multilayer confirms that the Ag nanoparticles form a monolayer near the surface of the DOPC membrane. Figure 1c shows the particle size distribution of the Ag nanoparticles whose average size is $5.4 \pm 2.3$ nm. Flexibility of the DOPC multilayer, which is in a liquid-crystalline state at room temperature, allowed penetration of Ag atoms and subsequent nucleation of particles within the layer. The limited diffusion rate of Ag atoms through the membrane, however, prevented coalescence of the nucleated particles and inhibited excessive growth, resulting in the observed discrete morphology. The formation mechanism of the Ag nanoparticles in the DOPC membrane is explained in detail elsewhere.[7]

It was shown by molecular dynamic simulation that the polar head groups of lipid molecules in a lipid bilayer will spontaneously bind to the incident metal nanoparticles.[11] Because the Ag nanoparticles are completely embedded within the lipid membrane, as can be seen in Figure 1b, based on the X-ray photoelectron spectroscopy (XPS) result, we infer that the Ag nanoparticles are indeed encapsulated by the chemically bound DOPC molecules. The Ag 3d XPS spectrum from the Ag particle-embedded lipid membrane is shown in Figure 2a. Both Ag $3d_{3/2}$ and $3d_{5/2}$ peaks contain shoulders at the lower binding energy side. Separation of the Ag $3d_{3/2}$ and $3d_{5/2}$ peaks (shown by dotted curves) reveals a small peak on each lower binding energy side of the Ag $3d_{3/2}$ and $3d_{5/2}$ peaks. These small peaks correspond to $Ag^{+}$.

Comparison of relative intensities of the metal and ionized peaks indicates that ≈20 mol% of Ag atoms are oxidized.[12] It is likely that Ag atoms on the surface of the nanoparticles are

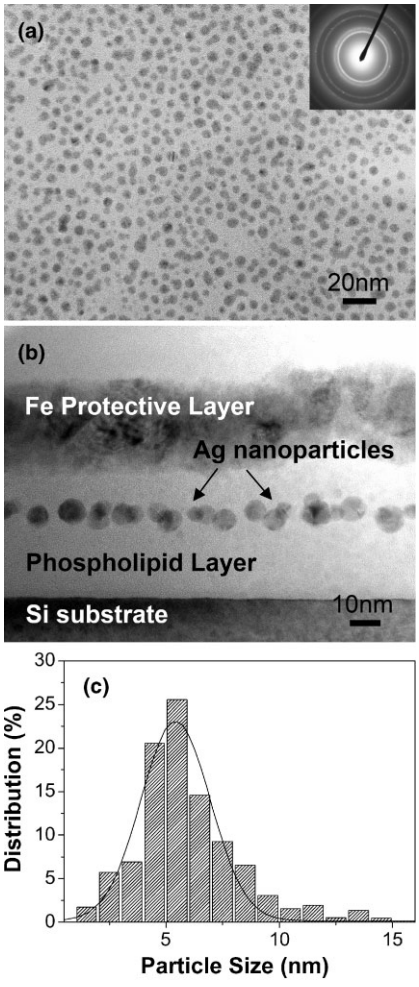


Figure 1. a) TEM plan-view image of the as-deposited Ag nanoparticles embedded in the DOPC multilayer. b) Cross-sectional TEM image of the as-deposited Ag nanoparticles. c) Particle-size distribution obtained from the TEM micrograph in (a).

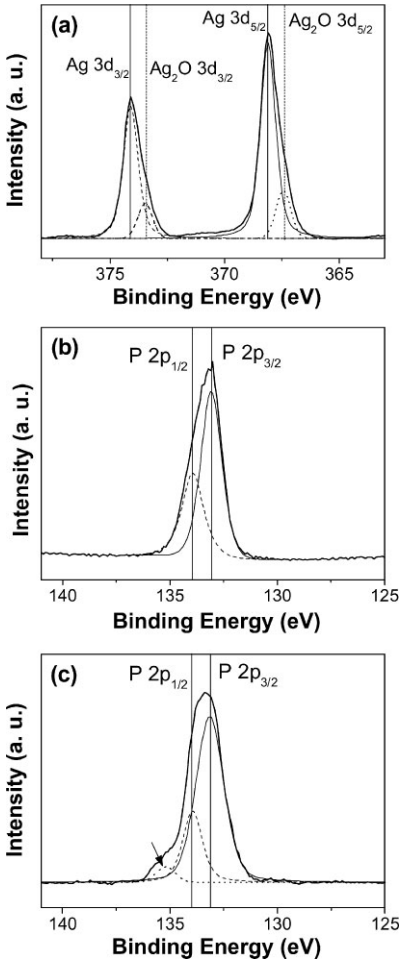


Figure 2. XPS spectra. a) Ag 3d spectrum from the Ag-embedded membrane. b) P 2p spectrum from DOPC membrane without Ag nanoparticles. c) P 2p spectrum from the Ag-embedded membrane (the arrow indicates the extra peak created due to the interaction of Ag atoms and DOPC head groups).

small NANO MICRO

chemically bound to the surrounding lipids. The P 2p XPS spectra obtained before and after the Ag deposition further confirm the chemical reaction between Ag and the lipid molecules. Prior to the Ag deposition, the P 2p spectrum exhibits a single peak at 133.3 eV (separated into P $2p_{1/2}$ and P $2p_{3/2}$ peaks), which corresponds well to the phosphate moiety of the phosphocholine head group of the phospholipid.[13] After deposition of Ag, a shoulder develops at 135.3 eV (marked by an arrow), which is indicative of chemical bonding resulting from the interaction of the DOPC head group and Ag atoms. The XPS result thus indicates that the lipids are most likely chemically bound to the Ag particle surface. This has significant implications regarding the tenability of Ag particle geometry as it would expedite the mass transfer of Ag atoms through the relatively high lateral mobility of lipids. If the lipid molecules are allowed to rearrange into a different conformation, we would expect a change in Ag particle morphology as a substantial fraction of Ag atoms are chemically bound to the lipid molecules.

The Ag-embedded DOPC membrane was hydrated to induce a structural change in the lipid multilayer as a DOPC multilayer tends to swell and form lipid rings with increasing water uptake.[14] Figure 3a shows typical UV–Vis spectra obtained immediately after the deposition of Ag on the DOPC versus after placing the Ag-embedded DOPC membrane in 100% relative humidity (in a desiccator saturated with water vapor) at room temperature for periods of 10 and 60 min. The spectrum from the as-deposited DOPC membrane contains a broad extinction band centered at 432 nm with a full-width-half-maximum of ≈84 nm. The extinction band arose from the surface plasmon resonance of Ag nanoparticles, which is a characteristic feature of nanosized Ag nanoparticles.[15] As the DOPC membrane is hydrated, the resonance peak is increasingly broadened and also red-shifted. In fact, the change in the spectrum was also verified visually as the sample surface color gradually changed from yellowish red to bluish black during hydration. Because the position and width of the surface plasmon resonance peak are directly correlated to the average particle size, distribution, and interparticle spacing, the change in the spectrum provides direct evidence for the morphological changes of the embedded Ag nanoparticles.

In order to examine the Ag nanoparticles with TEM with minimal interference, the DOPC multilayer was directly prepared on a TEM Cu grid coated with amorphous carbon thin film onto which Ag was deposited. The TEM image of the DOPC membrane after hydration for 10 min is shown in Figure 3b, which indicates that there was a significant change in the morphology of the Ag nanoparticles while the island-like discrete structure was still preserved. Compared to the TEM image for the as-prepared Ag particles shown in Figure 1a, the particles have coarsened dramatically by a factor of ≈100%, leading to a clearly visible change in the particle size distribution (Figure 3c). The average particle size increased from $5.4 \pm 2.3$ nm to $10.4 \pm 6.5$ nm after hydrating the sample for just 10 min. Our interpretation is that since the hydration was carried out at room temperature for a relatively short period, it is unlikely that the Ag nanoparticles coarsened through solid-state diffusion of neutral Ag atoms through the membrane. Since the lipid molecules have relatively high

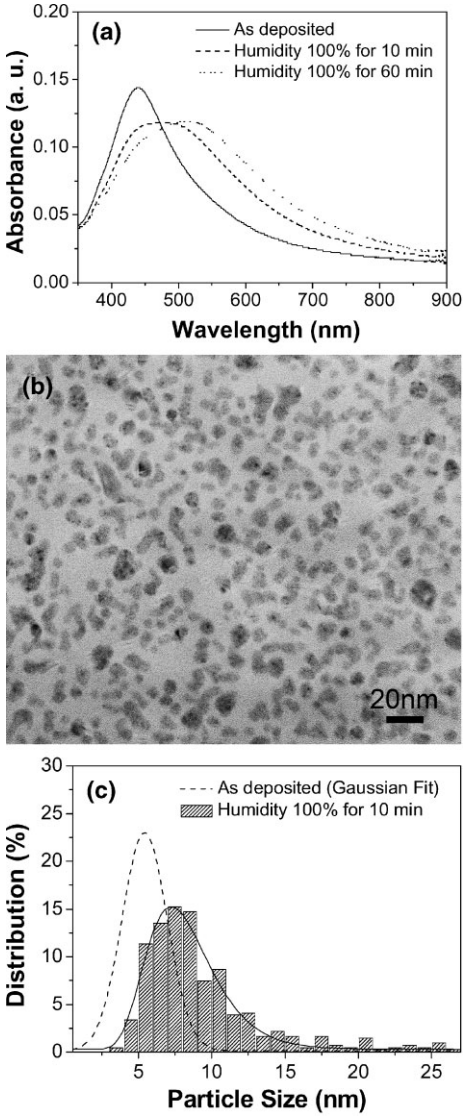


**Figure 3.** a) UV–Vis spectra of Ag nanoparticles embedded in the DOPC membrane before and after hydration. b) TEM plan-view image of the Ag-embedded DOPC membrane after hydration for 10 min. c) Particle-size distribution obtained from the TEM micrograph in (b).

lateral mobility, it is more likely that the mass transfer of Ag occurred via highly mobile lipid molecules chemically bound to Ag. The lateral diffusion coefficient of the head group in a phosphocholine lipid is estimated to be $2 \times 10^{-11}$ $m^2$ $s^{-1}$, which will give a typical diffusion length scale of 100 μm.[16] Such a high lateral diffusion rate corroborates that both size and shape of the individual Ag particles were rather easily altered by the migration of the lipid head group chemically bound to Ag.

As a comparison, when 3-nm-thick Au was deposited on the DOPC membrane instead of Ag, similarly sized Au nanoparticles were observed in the membrane, but unlike the case of Ag, the Au nanoparticles remained unchanged in their size when the membrane was hydrated for 12 h in 100% relative humidity as can be seen from Figure 4a. UV–Vis spectra obtained before and after hydration are also shown in Figure 4b. In agreement with the TEM data, no change in the

  

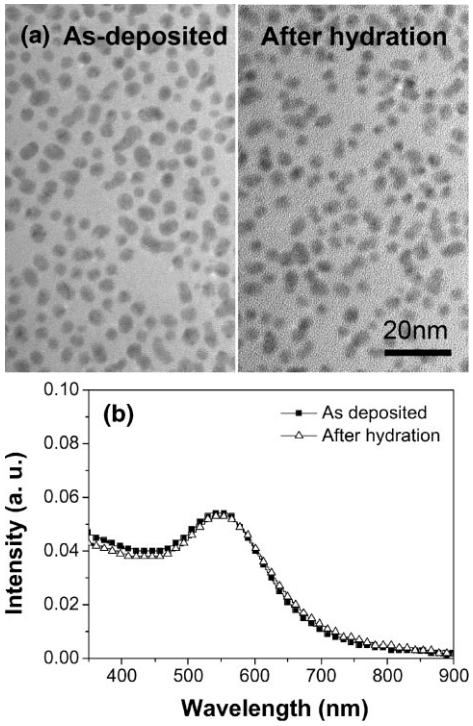


Figure 4. a) TEM plan-view image of the Au-embedded DOPC membrane before and after hydration for 12 h. b) UV–Vis spectra of Au nanoparticles embedded in the DOPC membrane before and after hydration.

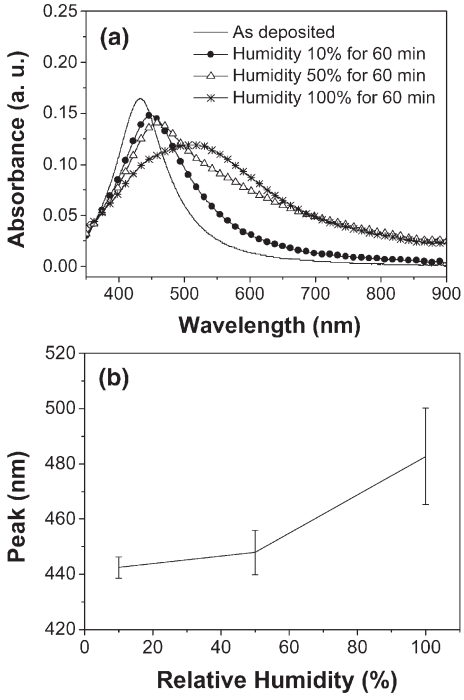


Figure 5. a) UV–Vis spectra of the Ag-nanoparticle-embedded DOPC membrane after hydration at different levels of relative humidity for 60 min. b) Plot of the peak position of the surface plasmon spectrum obtained at different levels of relative humidity for 60 min against the relative humidity.

spectrum is observed for the Au nanoparticles. XPS analysis of the Au-embedded DOPC membrane (see Supporting Information) verified that, unlike Ag, there was no change in chemical states. This result may indicate that chemical bonding did not develop between Au and the DOPC molecules. Therefore, it is concluded that chemical binding of the metal particles and the lipid molecules is a prerequisite to inducing spontaneous and fast morphological changes of the nanoparticles via rapid mobility of the lipid molecules.

In order to examine the sensitivity of the Ag-nanoparticle-embedded lipid membrane to different levels of humidity, the Ag-nanoparticle-embedded lipid membrane was subjected to 10% and 50% relative humidity for 60 min and the resulting UV–Vis absorption spectra are shown in Figure 5a. The spectrum clearly red-shifts and broadens with the increasing humidity level. The estimated position of the surface plasmon peaks is plotted against the humidity level in Figure 5b. The plot indicates that the Ag-nanoparticle-embedded lipid membrane is reasonably sensitive to detecting the presence of moisture in the atmosphere.

The change in the Ag-nanoparticle morphology was found to be reversible. When the hydrated sample was kept in an oven at 80 °C for dehydration, we observed that the Ag nanoparticles gradually reverted back to the original particle size distribution, as can be seen from the UV–Vis spectra in Figure 6a. When the Ag-nanoparticle-embedded membrane was dehydrated after being kept in a fully saturated atmosphere for 60 min, the resonance peak for Ag particles nearly returns to its original peak shape prior to hydration, and the peak width also decreased, indicating that the size of the Ag nanoparticles most likely returned to the original morphology with a narrowed size distribution. For visual evidence, a TEM image of the dehydrated sample is provided in Figure 6b. The TEM image shows that particles reattained their spherical shape with no presence of the interconnected particles. The image also contains several abnormally large particles, but these particles are a likely product of oxidation. The average particle size decreases from 10 nm when hydrated to $7.5 \pm 2.3$ after dehydration. In some regions, a large cluster of oxide particles was found as the dehydration was carried out at 80 °C after saturation. A control experiment was also performed by heating the Ag-nanoparticle-embedded membrane in vacuum with no water. No visible change in color or in the UV–Vis spectrum was observed in the sample after the heat treatment in a dry atmosphere. The reversible visual change in the color of the Ag-nanoparticle-embedded lipid membrane is detected only when water vapor is present in the atmosphere. To see whether the reversibility extends beyond the first cycle, the sample was repeatedly subjected to hydration/dehydration cycles. The hydration was carried out at room temperature, while the dehydration was done at 80 °C in vacuum in order to minimize the oxidation of the Ag nanoparticles. Figure 6c shows the UV–Vis spectra obtained after each hydration and dehydration step. After exhibiting a flat plateau with decreased intensity when hydrated, the spectrum reverted back to a narrow peak centered around 460 nm, similar to Figure 6a. However, the peak intensity somewhat progressively decreases due to the oxidation of Ag nanoparticles from repeated exposure to the humid environment. From Figure 6c it is evident that for up to 4 cycles there is truly a reversible

  

small NANO MICRO

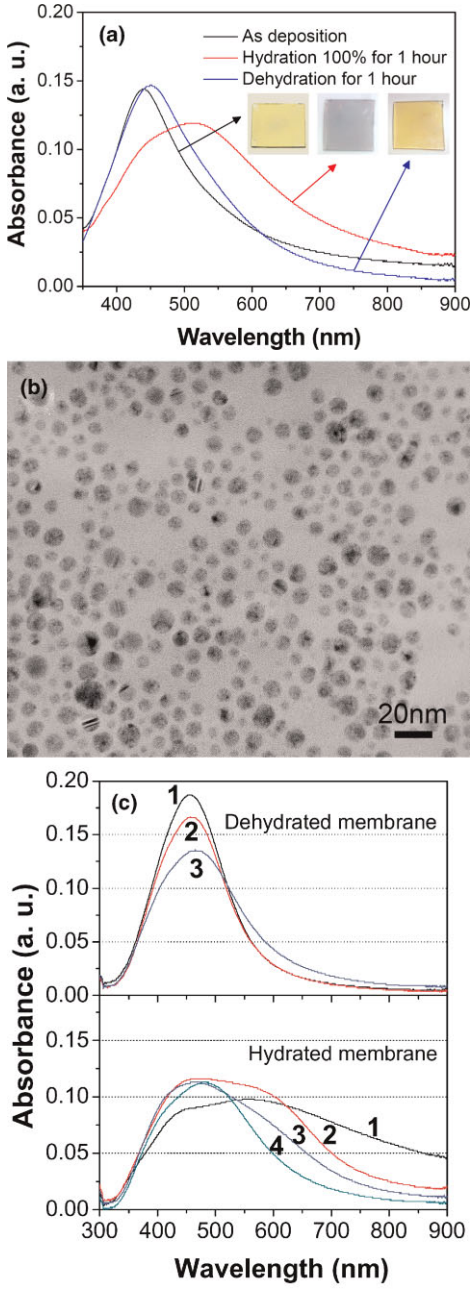


**Figure 6.** a) UV–Vis spectra of the Ag-nanoparticle-embedded DOPC membrane after hydration and after dehydration at 80 °C for 60 min. b) TEM plan-view image of Ag nanoparticles embedded in the DOPC membrane after dehydration for 60 min. c) UV–Vis spectra from the Ag nanoparticles embedded in the DOPC membrane obtained after each hydration/dehydration-in-vacuum cycle.

particle size change induced by the high mobility of lipid molecules.

It is noted that some interesting secondary structures other than a uniform monolayer can also be developed during dehydration of the membrane. During dehydration, the lipid membrane formed vesicles and domains of multilayers normal to the membrane instead of returning to the original aligned multilayer structure. Hence, we found regions in which the Ag nanoparticles were arranged into a circular structure

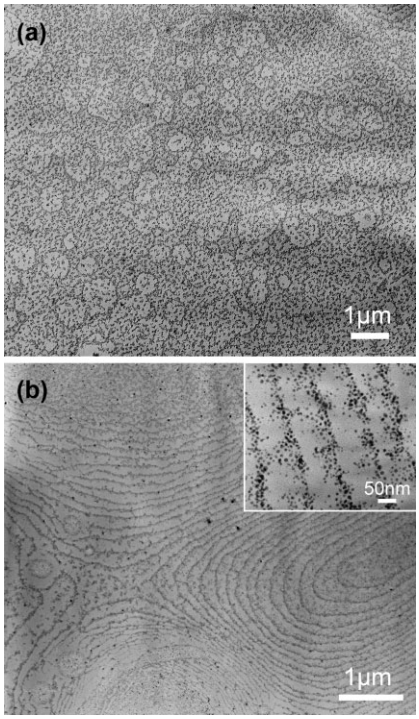


**Figure 7.** TEM plan-view images of the Ag-nanoparticle-embedded DOPC membrane after dehydration at 80 °C for 60 min. a) Region showing a vesicular superstructure. b) Region showing a parallel wavy superstructure. The inset shows the magnified image of the wavy lines.

surrounded by a ring, devoid of nanoparticles, resulting from a vesicular arrangement of the lipid molecules (Figure 7a). In other areas (Figure 7b), the Ag nanoparticles were arranged into long parallel wavy strips likely to be generated by multilayer domains created in the membrane. The magnified image of the parallel strips, shown as the inset in Figure 7b, clearly shows the Ag nanoparticles arranged in parallel lines. Although the Ag nanoparticles were arranged in different configurations depending on the lipid structure, the particle size was still found to be relatively uniform.

Because the Ag nanoparticles embedded in the DOPC membrane almost instantaneously produce visually detectable color changes in the membrane when hydrated by moisture, the nanoparticles-in-lipid structure could potentially be used as a sensor for detecting moisture in the atmosphere. Similar color changes in the lipid-embedded-Ag-nanoparticle sample were also produced by volatile organic solvents such as methanol, so the lipid–nanoparticle composite system can be utilized as a sensor for various organic solvents.

In order to probe the structural change incurred by the Ag-nanoparticle-embedded DOPC membrane during hydration and dehydration, the surface structure of the lipid membrane was examined with atomic force microscopy (AFM). AFM analysis of the as-prepared and hydrated lipid membrane without Ag nanoparticles revealed no visible change in surface morphology during hydration, indicating that the lipid multilayer swells up, maintaining a flat surface without the embedded Ag nanoparticles (see Supporting Information). When Ag nanoparticles are embedded within the lipid membrane, a marked change in surface morphology is

observed. Instead of a flat surface, the surface of the Ag-nanoparticle-embedded lipid membrane contains a grainy surface texture (Figure 8a). It is conjectured that the Ag nanoparticles embedded underneath the membrane surface created the ripple-like surface roughness. As the lipid membrane is saturated with water vapor for 60 min, the AFM image in Figure 8b shows a huge increase in surface roughness due to the appearance of two different structures. The hydrated membrane contains protruding regions that exhibit very fine surface roughness. These areas are believed to contain Ag nanoparticles. As can be seen from the line profiles in Figure 8c, the roughness has become much finer in pitch with hydration. The hydrated membrane also contains flat regions devoid of such fine surface roughness. The observation suggests that Ag nanoparticles are forced together during hydration, forming regions in which Ag nanoparticles cluster together. The regions in which Ag nanoparticles are driven away become flat and free of the embedded nanoparticles. Clustering of the Ag nanoparticles causes the particle size to increase and the interparticle distance to decrease, leading to the red-shift of the surface plasmon peak. When the hydrated membrane is dehydrated at 80 °C, the membrane reverts back to the flat morphology (Figure 8d). The reversible change in the lipid membrane appears to stem from the peculiar swelling behavior with presence of the Ag nanoparticles. The reason for the altered swelling behavior in presence of Ag nanoparticles is not clear, however, it is speculated that the Ag-nanoparticle-embedded DOPC membrane is in a metastable state and lipid molecules around the Ag nanoparticles exist as a highly curved bilayer. Uptake of the water molecules appears to trigger nonuniform swelling of the lipid multilayer, accentuating the preexisting undulation.

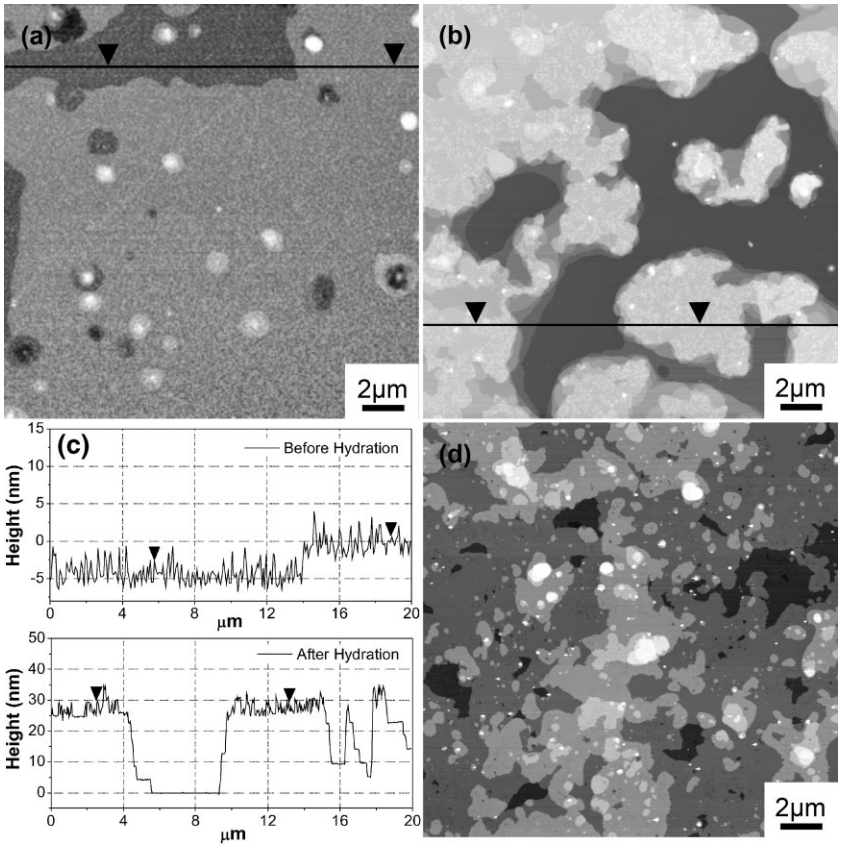


**Figure 8.** AFM images of the Ag-nanoparticle-embedded DOPC membrane. a) As-prepared. b) After hydration for 60 min in 100% relative humidity. c) Line profiles from the marked lines in (a) and (b). d) After dehydration at 80 °C for 60 min.

Lastly, we also carried out an X-ray reflectivity (XRR) analysis on the Ag-nanoparticle-embedded membrane in order to discern the structural changes observed during hydration/dehydration of the lipid membrane. The result shown in Figure 9 demonstrates a highly ordered vertical structure of the lipid multilayer prior to the Ag deposition. The bilayer spacing calculated from the Bragg peaks is 5 nm, indicating that the multilayer was composed of 14 DOPC bilayers. After the Ag deposition, disturbance of the lipid stacking order slightly dampened the Kiessig fringes. When hydrated, the Kiessig fringes further dampened and completely disappeared after 2 h in a fully saturated humidity environment. After dehydration, no visible Kiessig fringes were detected, which is reasonable since the multilayer did not entirely return to its original aligned form when dehydrated (Figure 9). The bilayer spacing summarized in Table 1

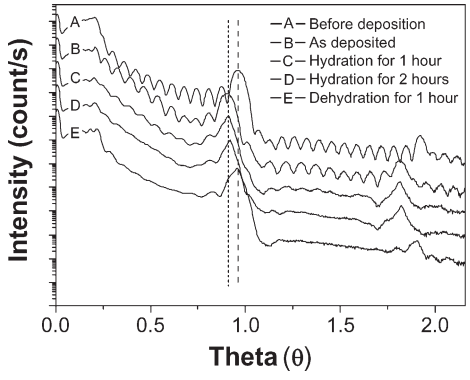


**Figure 9.** XRR spectra from the DOPC membrane and Ag-nanoparticle-embedded DOPC membrane during hydration and dehydration.

**Table 1.** Bilayer spacing analyzed with XRR during hydration/dehydration of the lipid membrane.

| | Before Ag Deposition | After Ag Deposition | Hydration for 1 hour | Hydration for 2 hours | After Dehydration |
|---|---|---|---|---|---|
| Bilayer Spacing [nm] | 4.62 ± 0.044 | 4.83 ± 0.079 | 4.89 ± 0.002 | 4.91 ± 0.040 | 4.66 ± 0.006 |

small NANO MICRO



indicates that the DOPC multilayer swells up with increasing moisture content and reverts back when dehydrated. Hence, changes in the DOPC structure during the hydration/dehydration cycle are consistent with reversible morphological changes observed in the embedded Ag nanoparticles, further supporting the view that mobility of the lipid molecules is responsible for the morphological changes of the Ag nanoparticles.

## 3. Conclusions

We demonstrated that the Ag nanoparticles embedded in a liquid-crystalline lipid membrane undergo a reversible morphological change, mediated by the rapid mobility of lipid molecules during the phase transition. The morphological change occurred on a time scale that enables the Ag-nanoparticle-embedded membrane to be used as a visual sensor for detecting moisture as well as other organic solvents. Because of the biocompatibility of the lipid molecules, biomolecule-triggered phase changes in the lipid structure could also lead to morphological alteration of the embedded Ag nanoparticles, rendering the Ag-nanoparticle-in-lipid membrane a potential candidate system for biosensing.

## 4. Experimental Section

The solid-supported DOPC membrane was prepared by spin-coating the lipid solution onto a Si (or fused silica) substrate following the method devised by Mennicke and Salditt.[10] The lipid solution was made by dissolving the DOPC lipids in chloroform (10 mg $mL^{-1}$). 100 μL of lipid solution was used to form the multilayer by spin-coating the lipid solution at 5000 rpm onto a 2 cm × 2 cm substrate. After spin-coating, the solvent was allowed to evaporate in a freeze dryer for 12 h. A 3-nm-thick Ag layer was deposited onto the lipid multilayer using a thermal evaporator. The film thickness was monitored using a quartz balance.

TEM (JEOL2010), AFM (XE-100 from PSI), and UV–Vis spectrophotometry (UV-2450 from SHIMADZU) were used to characterize the Ag-embedded lipid membrane. For preparing the TEM specimen, the lipid multilayer spin-coating and Ag deposition was carried out directly onto a TEM Cu grid covered by amorphous carbon film. The lipid multilayer on the Cu grid was electron-transparent so that TEM observation was made without any further treatment. For cross-sectional TEM samples, a 30-nm-thick Fe film was deposited on the lipid membrane to seal and protect the sample from damage during the TEM sample preparation. After capping the sample, the normal TEM sample preparation procedure was followed, which includes gluing of two samples, cutting, grinding, and ion milling. For XPS (PHI 5800), monochromatic X-rays generated from Al K$\alpha$ (14.7 kV, 33 mA) with beam size of 1 μm × 4 μm were used to study structural changes in the Ag-embedded lipid membrane. (XRR (X'pert PRO from PANalytical) measurements were carried out at room temperature using Cu K$\alpha$ radiation with wavelengths $\lambda_{K\alpha 1} = 1.5406$ Å and $\lambda_{K\alpha 2} = 1.5444$ Å and the intensity ratio was 2:1.

## Acknowledgements

*This work was supported by the Ministry of Science and Technology through the Nanoscopia Center of Excellence at Hanyang University.*

[1] M. Uchida, M. T. Klem, M. Allen, P. Suci, M. Flenniken, E. Gillitzer, Z. Varpness, L. O. Liepold, M. Young, T. Douglas, *Adv. Mater.* **2007**, *19*, 1025.
[2] D. M. Small, in *The Physical Chemistry of Lipids, Handbook of Lipid Research*, Vol. *4*, Plenum, New York 1986.
[3] A. Terheiden, B. Rellinghaus, S. Stappert, M. Acet, C. Mayer, *J. Chem. Phys.* **2004**, *121*, 510.
[4] B. Yang, S. Kamiya, K. Yoshida, T. Shimizu, *Chem. Commun.* **2004**, 500.
[5] J. H. Jung, G. John, K. Yoshida, T. Shimizu, *J. Am. Chem. Soc.* **2002**, *124*, 10674.
[6] A. Terheiden, C. Mayer, K. Moh, B. Stahlmecke, S. Stappert, M. Acet, B. Rellinghaus, *Appl. Phys. Lett.* **2004**, *84*, 3891.
[7] N. Oh, J. H. Kim, C. S. Yoon, *Adv. Mater.* **2008**, *20*, 3404.
[8] A. Terheiden, B. Rellinghaus, M. Acet, C. Mayer, *Phase Transitions* **2005**, *78*, 25.
[9] C. A. Veracini, D. Catalano, in *The Molecular Dynamics of Liquid Crystals*, NATO ASI Series C, Vol. *431*, (Eds: G. R. Luckhurst, C. A. Veracini), Kluwer Academic Publishers, Dordrecht, The Netherlands **1994**, Ch. 20.
[10] U. Mennicke, T. Salditt, *Langmuir* **2002**, *18*, 8172.
[11] V. V. Ginzburg, S. Balijepalli, *Nano Lett.* **2007**, *7*, 3716.
[12] J. F. Weaver, G. B. Hoflund, *Chem. Mater.* **1994**, *6*, 1639.
[13] W. M. Heckl, K. M. R. Kallury, M. Thompson, C. Gerber, H. J. K. Horber, G. Binnig, *Langmuir* **1989**, *5*, 1433.
[14] J. Thimmel, B. Klösgen, W. Helfrich, G. Rapp, in *Perspectives in Supramolecular Chemistry: Giant vesicles*, Vol. *6*, (Eds: P. L. Luisi, P. Walde), John Wiley & Sons, Chichester, England **2000**, Ch. 18.
[15] S. He, J. Yao, P. Jiang, D. Shi, H. Zhang, S. Xie, S. Pang, H. Gao, *Langmuir* **2001**, *17*, 1571.
[16] D. P. Tieleman, S. J. Marrink, H. J. C. Berendsen, *Biochim. Biophys. Acta* **1997**, *1331*, 235.

Received: October 10, 2008
Revised: December 11, 2008
Published online: March 9, 2009

  